Construction and Building Materials 329 (2022) 127106

Contents lists available at ScienceDirect

Construction and Building Materials

journal homepage: www.elsevier.com/locate/conbuildmat

Thermo-piezo-rheological characterization of asphalt concrete

Mequanent Mulugeta Alamnie [a,*], Ephrem Taddesse [a], Inge Hoff [b]

[a] Department of Engineering Science, University of Agder, 4879 Grimstad, Norway
[b] Department of Civil and Environmental Engineering, Norwegian University of Science and Technology (NTNU), Høgskoleringen 7a, Trondheim, Norway

ARTICLE INFO

Keywords:
Thermo-piezo-rheology
Linear viscoelastic
Triaxial dynamic modulus
Relaxation modulus
Triaxiality ratio
Asphalt concrete

ABSTRACT

The linear viscoelastic (LVE) properties of asphalt concrete is investigated in this paper using a controlled-strain triaxial dynamic modulus test over wide frequency, temperature, and confining pressure ranges. The time–temperature-pressure superposition principle (TTPSP) is applied to validate the thermo-piezo-rheological simplicity of the tested materials using triaxial master curves. The LVE response is found highly stress-dependent at intermediate and high temperatures. The Prony series modeling of time-domain properties ascertains that confining pressure strongly correlates with long-term relaxation modulus, the absolute maximum slope of the relaxation modulus, and viscoelastic damage parameter. The stress triaxiality ratio concept is applied, and a new shift model is proposed that takes the triaxiality ratio as an internal state variable in the TTPSP. The model prediction agrees well with the experimental data. Moreover, a relationship between the long-term relaxation modulus and the triaxiality ratio is established. The triaxiality ratio coupled with TTPSP can accurately describe the stress-dependent response of asphalt concrete in the LVE domain.

1. Introduction

Asphalt concrete is a composite, time-dependent material that exhibits elements of elastic, viscous, and viscoelastic properties. The response of such materials is dependent on loading frequencies and a set of thermodynamic variables. As a fundamental thermodynamic variable, temperature and pressure significantly influence the viscoelastic and viscoplastic responses of time-dependent materials. The effect of time (frequency) and temperature is characterized using a joint parameter called reduced time (or reduced frequency) for a thermo-rheological simple material. Similarly, a time-pressure shift factor is used to analyze the joint effect of time and pressure for the piezo-rheological simple material. Several researchers have validated that the thermo-rheological simplicity (time–temperature response) of different asphalt concrete mixtures and the applicability of time–temperature superposition principle (TTSP) in both undamaged and damaged states [3,20,29,26,14]. The validity of TTSP in undamaged and damaged states yields a significant material saving for the test [5]. The combined effect of the two fundamental thermodynamic variables (temperature and pressure) on the viscoelastic response is described using the Time-Temperature-Pressure superposition principle (TTPSP). A material that satisfies the TTPSP principle is called a *thermo–piezo-rheological simple* material [23,6]. The role of confining pressure on time-dependent materials has also been studied for several decades, such as for polymers [8,12]. As a three-phase material, asphalt concrete showed strong stress-dependent properties. Most studies on the triaxial stress response of asphalt concrete were focused on the viscoplastic properties [2,1,19,24]. Some studies such as Yun et al.[26] and Rahmani et al.[18] have investigated the role of confinement on the applicability of TTSP with growing damage and the effect of confining pressure on Schapery's nonlinear viscoelastic parameters, respectively. Other studies [28,29,21] have investigated the effect of confining pressure on linear viscoelastic (LVE) responses of asphalt concrete mixtures using triaxial master curves. Previous research focused on proposing 'vertical' shift models as a function of confining pressure and was mainly involved in constructing the 'triaxial' master curves. The triaxial stress evolution in the LVE range was not discussed in previous research. Furthermore, most standards typically use uniaxial dynamic modulus tests for asphalt concrete LVE properties, including the mechanistic-empirical pavement analysis methods. However, the triaxial (confined) dynamic modulus test is more realistic to simulate the in-situ condition and the stress-dependent LVE properties should be investigated for accurate characterization of asphalt concrete.

In this paper, strain-controlled triaxial dynamic modulus tests were conducted at wide ranges of confining pressure (0 to 300 kPa), temperature (-10 to 55 °C), and frequency (20 to 0.1 Hz). A target on-

* Corresponding author.
E-mail addresses: mequanent.m.alamnie@uia.no (M. Mulugeta Alamnie), ephrem.taddesse@uia.no (E. Taddesse), inge.hoff@ntnu.no (I. Hoff).

https://doi.org/10.1016/j.conbuildmat.2022.127106
Received 5 August 2021; Received in revised form 31 January 2022; Accepted 8 March 2022
Available online 16 March 2022

specimen strain magnitude of less than or equal to 50 micros is selected to ensure that the deformation due to sinusoidal stress is within the LVE domain. A test procedure was proposed in the experimental campaign, and two different asphalt mixtures were tested. The main objective of this research is to investigate the stress-dependent LVE properties of asphalt concrete using the triaxial dynamic modulus test and develop a simplified triaxial shift model. The objective is achieved; first by verifying the *thermo-piezo-rheological simplicity* of the tested materials (constructing triaxaial dynamic modulus master curves using existing and new triaxial shift models), and second by investigating the stress-dependent time-domain LVE properties using the Prony method. Furthermore, the role of confinement was also explored on the maximum slope of relaxation modulus and the viscoelastic damage parameter. Finally, the triaxiality ratio concept is introduced to analyze the triaxial (3D) stress-state on the LVE responses of asphalt concrete. A new triaxial shifting model is proposed using the triaxiality ratio as an internal state variable and validated using experimental data. Moreover, a simplified model is established between the long-term relaxation modulus and the triaxiality ratio to explain the stress-dependent viscoelastic behaviors of asphalt concrete. Unless otherwise stated, the term pressure in this paper refers to confining pressure (stress).

2. Viscoelasticity

The uniaxial stress–strain constitutive relationship for linear viscoelastic (LVE) material can be expressed in a Boltzmann superposition integral form in the time domain.

$$\sigma(t) = \int_0^t E(t-\tau)\frac{d\varepsilon}{d\tau}d\tau \tag{1}$$

Where σ and ε are stress and strain, respectively; t is physical time; τ is integral variable; $E(t)$ is relaxation modulus. The one-dimensional relaxation modulus, $E(t)$ is commonly expressed using a generalized Maxwell mechanical model (GM in parallel) with the Prony series.

$$E(t) = E_\infty + \sum_{m=1}^{M} E_m\left[e^{(-t/\rho_m)}\right] \tag{2}$$

Where E_∞ is Long-term (equilibrium) modulus; E_m is components of the relaxation modulus; ρ_m is components of relaxation time; and M is the total number of the Maxwell elements (one Maxwell element is composed of one elastic spring and one viscous dashpot connected in series). For generalizations into 3D formulations, the deformations within a material can be decoupled into shear and volumetric components. The time-dependent stress–strain response of an isotropic LVE material in 3D can thus be described in both deviatoric (G(t)) and bulk or volumetric (K(t)) relaxation moduli, as follow.

$$G(t) = G_\infty + \sum_{m=1}^{M} G_m\left[e^{\left(-t/\rho_{m,G}\right)}\right] \tag{3}$$

$$K(t) = K_\infty + \sum_{n=1}^{N} K_n\left[e^{\left(-t/\rho_{n,K}\right)}\right] \tag{4}$$

Where G_∞ and K_∞ are Long term (equilibrium) shear and bulk moduli,G_m, $\rho_{m,G}$ and K_n, $\rho_{n,K}$ are Prony coefficients of relaxation modulus and time for shear and bulk, respectively. M and N are the number of Prony coefficients for shear and bulk relaxation. It is generally assumed as $\rho_{m,G} = \rho_{n,K} = \rho_m$. For the small stress LVE test, the time-dependent volumetric deformation of asphalt concrete is negligible. The reasons include (i) the hydrostatic pressure is usually less than the material's tensile strength that causes a linear elastic volumetric deformation, (ii) K (t) is very high and viscous flow is assumed isochronous (linear flow). Hence, the time-dependent volume change is much smaller than the corresponding shear distortion on the same material [9] and a constant Poisson ratio (υ) is often assumed for asphalt concrete.

$$K(t) = \frac{E(t)}{3(1-2\upsilon)}, \quad G(t) = \frac{E(t)}{2(1+\upsilon)} \tag{5}$$

In theory, the relationships between the three moduli (K(t), G(t), and E(t)) should be established using a time-dependent Poisson's ratio [27,17].

Table 1
Aggregate gradation.

Sieve size [mm]	AB11 [%]	SKA11 [%]
16.0	100	100
11.2	95	91.2
8.0	70	53.6
4.0	48	35.7
2.0	36	21.7
0.25	15.5	12.8
0.063	10	8.4
Binder Content [%]	5.6	5.83

3. Materials and test method

3.1. Materials

In this study, two different asphalt concrete mixtures (AB11 and SKA11) collected from asphalt concrete production plants were used. The AB11 mixture is dense-graded asphalt concrete and SKA11 is a stone mastic asphalt. Both mixes have an 11 mm nominal maximum aggregate size (NMAS), where AB11 is a polymer-modified (PMB 65/105–60) while SKA11 is a 70/100 neat binder mixture. The gradation is given in Table 1. Cylindrical samples were produced by re-heating the loose mix at 150 °C for up to 4 h and compacting using a gyratory compactor according to the Superpave specification. The final test specimens (Ø100 mm and 150 mm height) were fabricated by coring and cutting from the Ø 150 mm and 180 mm height samples.

3.2. Test procedure

A triaxial dynamic modulus test was performed using a servo-hydraulic universal testing machine (IPC UTM-130). Three sets of loose core linear variable differential transducers (LVDTs) were mounted on the specimen at 120°apart radially with 70 mm gauge length. The instrumented specimens were conditioned at a target temperature for at least 2 h. A strain-controlled sinusoidal compressive load was applied axially with a target on-specimen axial strain of 50 micros or less. The test was conducted according to AASHTO T378 over a wide range of temperatures (-10, 5, 21, 40, 55 °C), pressures (0, 10, 100, 200, 300 kPa) and frequencies (20, 10, 5, 2, 1, 0.5, 0.2, 0.1 Hz). Three specimen replicates were tested at each temperature and pressure according to the following steps.

(1). The instrumented sample is installed in the testing system at the target temperature. A sinusoidal load is applied from high to low frequencies without a rest period between sweeps. The average strain of three LVDTs should not be more than the target 50 micros.
(2). Then, 10 kPa confining pressure is applied for about 15 min to stabilize the deformation due to confinement. Repeat step 1.
(3). Compare dynamic modulus and phase angle values from steps 1 (unconfined or uniaxial) and step 2 (10 kPa confined). The dynamic modulus results should not vary by a significant margin.
(4). Apply 100 kPa confining pressure (for 15 min). Repeat step 1.
(5). Apply 200 kPa confining pressure (for 15 min). Repeat step 1.
(6). Apply 300 kPa confining pressure (for 15 min). Repeat step 1.

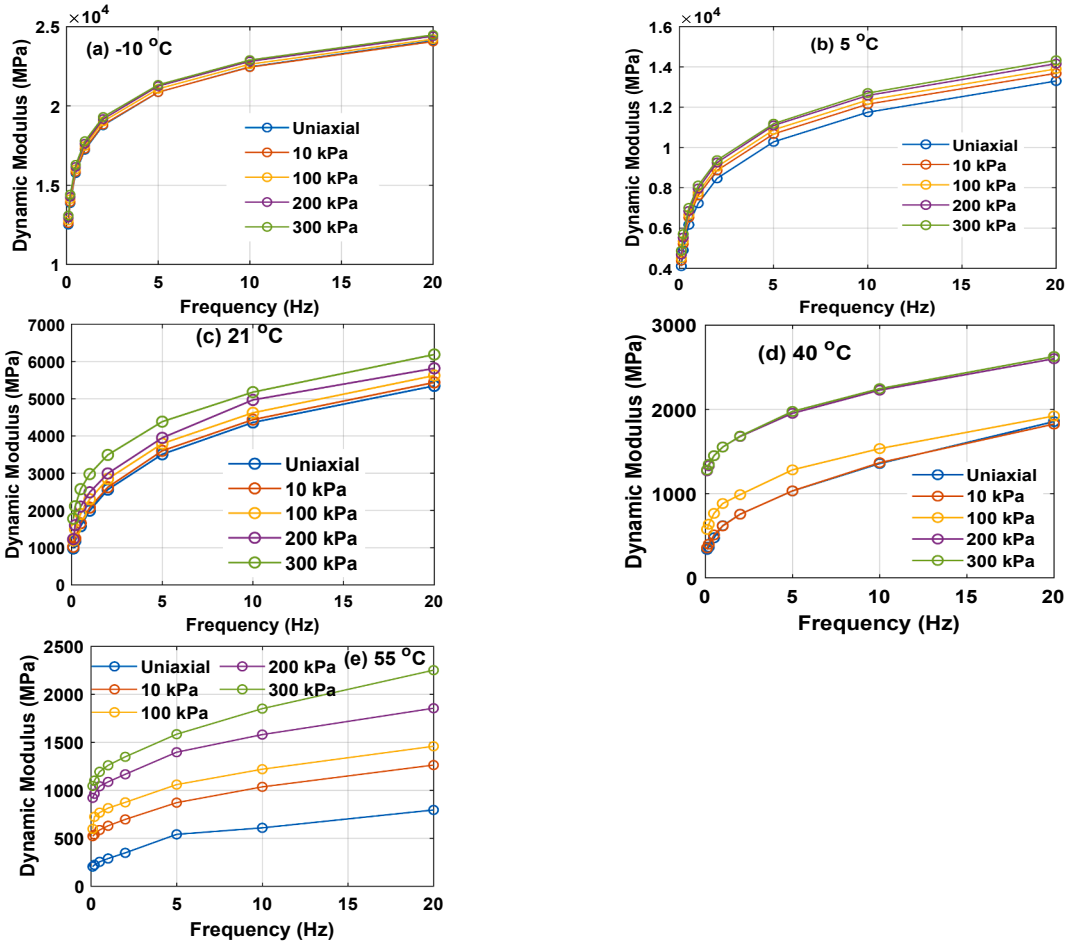

Fig. 1. Dynamic modulus at different temperatures and confining pressures - AB11 mixture.

4. Dynamic modulus test results

The response of an asphalt concrete material in a dynamic modulus test under a continuous sinusoidal loading is expressed by a complex modulus,E^*. The three measured parameters (outputs) strain $\varepsilon(t)$, stress $\sigma(t)$, and dynamic modulus, E^* are expressed as follows.

$$\varepsilon(t) = \varepsilon_o sin(\omega t) \tag{6}$$

$$\sigma(t) = \sigma_o sin(\omega t + \varphi) \tag{7}$$

$$E^* = \frac{\sigma_o e^{i(\omega t+\varphi)}}{\varepsilon_o e^{i\omega t}} = |E^*|(cos\varphi + isin\varphi) = |E^*|e^{i\varphi} \tag{8}$$

$|E^*|$ is the norm of dynamic modulus, $E' = |E^*|\cos\varphi$ and $E'' = |E^*|\sin\varphi$ are the storage and loss moduli, respectively, σ_o and ε_o are stress and strain amplitudes, respectively. The phase angle, φ [0, 90°] is calculated from time lag (t_i) in strain signal and loading period (t_p) of the stress signal,$\varphi = 360^o\left(\frac{t_i}{t_p}\right)$. A material with a phase angle between 0° (purely elastic) and 90° (purely viscous) is a viscoelastic material. The dynamic modulus test results are the average of modulus on three specimens at each temperature, confining pressure and frequency. The average specimen-to-specimen variation for dynamic modulus value is generally less than 10% at high temperatures (40 and 55 °C). The variation is overall less than 5% for lower temperatures (21, 5 and -10 °C).

4.1. Effect of confining pressure on dynamic modulus

The effect of confining stress on the viscoelastic response of asphalt concrete is investigated by conducting triaxial dynamic modulus tests. The triaxial dynamic modulus test results of the AB11 mixture are presented in Fig. 1 (a-e). It is clearly seen that confining pressure has a significant role on the viscoelastic response of asphalt concrete at intermediate (21 °C) and high temperatures (40 °C and 55 °C) but marginal or no effect at lower temperatures (such as 5 °C). For example, at 1 Hz frequency, the dynamic modulus at 300 kPa is 1.5 times (at 21 °C), 2.5 times (at 40 °C), and 4.4 times (at 55 °C) that of the uniaxial dynamic modulus. Moreover, the effect of confinement at 40 °C has some irregular patterns as compared to the dynamic moduli at 21 and 55 °C. The cause of such variations can be due to the increase in binder viscosity at high temperatures and low frequencies, resulting in a higher phase angle. However, the measured phase angles at higher temperatures are dictated not only by the binder but also by aggregate interactions. The binder becomes soft at high temperatures and low frequencies and the elastic aggregate structure dominates the mixture behavior, which is reflected by the reduction of phase angle. The role of confinement in such conditions is retarding the binder flow, and aggregate-to-aggregate contact is reduced. The other reason can be the transient effects during the dynamic modulus test [10], in addition to the microstructural change between 30 and 55 °C.

4.2. Isobaric master curves

The dynamic modulus test data are shifted horizontally (along the logarithmic frequency axis) to construct a master curve at a reference temperature using a sigmoidal function [16].

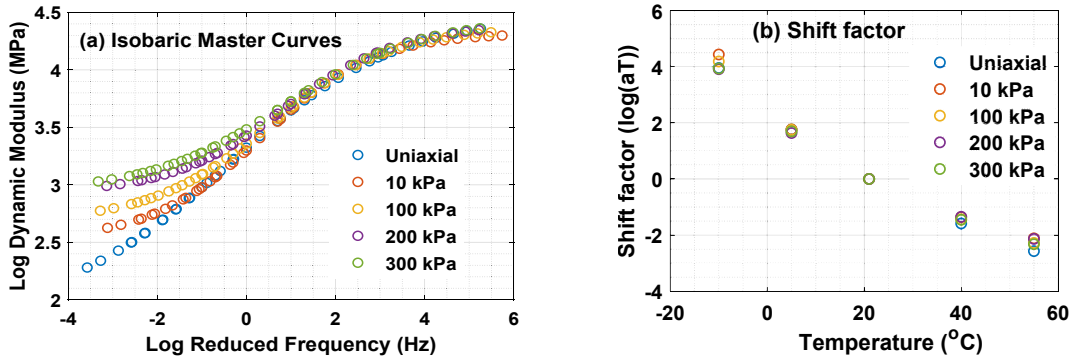

Fig. 2. Isobaric master curves and shift factors at 21 °C reference temperature – AB11 Mixture.

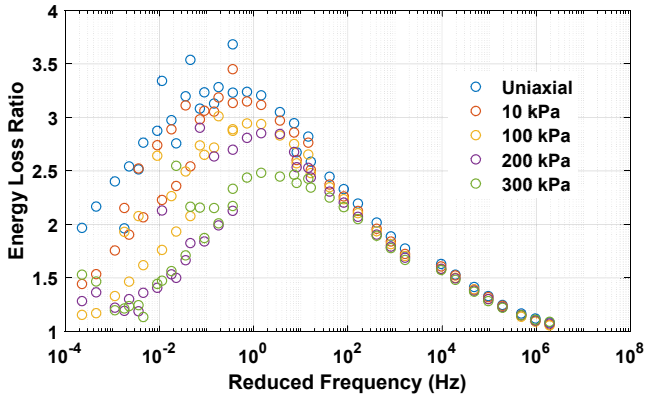

Fig. 3. Energy loss ratio (specific loss) at different confining stress levels – AB11 Mixture.

$$log(E^*) = \delta + \frac{(\alpha - \delta)}{1 + exp(\eta - \gamma log f_R)} \tag{9}$$

Where E^* is the dynamic modulus, δ and α are the minimum and maximum logarithm of the dynamic modulus, respectively, η and γ are shape factors and f_R is reduced frequency.

$$f_R = \alpha_T \times f \tag{10}$$

Where f is the frequency and a_T is time–temperature shift factor. The Williams, Landel, and Ferry (WLF) function [25] is widely used for a_T.

$$log\alpha_T = -\frac{C_1(T - T_0)}{C_2 + T - T_0} \tag{11}$$

Where C_1 and C_2 are WLF constants and T_0 is reference temperature. The isobaric master curves are constructed at 21 °C reference temperature using the sigmoid model and WLF shift function for the AB11 mixture, as shown in Fig. 2a. The isobaric master curves did not fall into a single curve at high temperatures (and low frequencies). The shift factors in Fig. 2b also showed a slight variation at different confining pressure levels. Moreover, the effect of confining pressure can be seen from the energy loss quantity during the dynamic modulus test. The total energy in cyclic viscoelastic deformation has a dissipated ($\Delta W = \pi\sigma_o\varepsilon_o sin\varphi$) and stored ($W = \frac{\sigma_o\varepsilon_o}{2}$) energy components in J/m^3 per cycle [22,9]. The ratio of dissipated energy to the maximum stored energy ($\frac{\Delta W}{W}$) is independent of stress and strain amplitudes, as shown in Eq. (12).

$$\frac{\Delta W}{W} = 2\pi \sin\varphi \tag{12}$$

As shown in Fig. 3, the maximum energy loss ratio is recorded around 0.1 Hz frequency. At this point, confining pressure contributed to reducing the dissipated energy (or phase angle) and confining pressure has no significant effect on energy loss at low temperatures and high frequencies. Therefore, confining pressure retarded energy loss and contributed to the elastic energy at high temperatures and low frequencies. These observations verify that the LVE properties of asphalt concrete are stress-dependent at intermediate and elevated temperatures. Hence, a stress-dependent shift function is necessary to generate a single, continuous master curve for LVE characterization in a triaxial stress state.

4.3. Stress-dependent master curve

In the triaxial dynamic modulus test, the confining pressure causes an increase of dynamic modulus. To construct a stress-dependent master curve, the modulus at different frequencies, confining pressures and temperatures are shifted both horizontally and vertically. The time–temperature shift factor is superposed and modified to couple pressure in the shifting function. Two models are suggested to construct and compare stress-dependent or triaxial master curves. The first model (Model-1) is the modified WLF function proposed by Fillers, Moonan, and Tschoegl (FMT) model [8], expressed as follows.

$$log\alpha_{TP} = \frac{-C_1(T - T_0 - \Gamma(p))}{C_2(P) + T - T_0 - \Gamma(p)} \tag{13}$$

$$\Gamma(p) = C_3(P) ln\frac{1 + C_4P}{1 + C_4P_0} - C_5(P) ln\frac{1 + C_6P}{1 + C_6P_0} \tag{14}$$

Where α_{TP} is time–temperature-pressure shift factor; P is the pressure of interest; P_0 is reference pressure;C_1, C_4 and C_6 are constants;$C_2(p)$, $C_3(p)$ and $C_5(p)$ are pressure-dependent parameters. In the FMT model, the coefficients represent the thermal expansion of the relative free volume and the pressure-dependent parameter $\Gamma(p)$ accounts for the compressibility attributed to the collapse of free volume [7]. The FMT equation can be reduced to the WLF equation at $P = P_o = 0$, and when$T = T_o$, the FMT function becomes a pressure shift function. A modified version of Model-1 is proposed in this paper. The pressure-dependent coefficients $C_2(P)$ and $C_3(P)$ are approximated as linear functions and the last component of Eq. (14) can be dropped.

$$\begin{aligned} C_2(P) &= C_{20} + C_{21}P, \\ C_3(P) &= C_{30} + C_{31}P \end{aligned} \tag{15}$$

Where $C_{20}, C_{21}, C_{30}, C_{31}$ are coefficients. The proposed modified FMT model (Model-1) time-pressure or "vertical" shift factor takes the following form.

$$\Gamma(p) = (C_{30} + C_{31}P) ln\frac{1 + C_4P}{1 + C_4P_0} \tag{16}$$

The second triaxial shifting model (Model-2) is a sigmoid-type Zhao's model [30], expressed as,

$$log\lambda = \frac{-(P - P_o)}{exp[C_3 + C_4 log(f_R)] + C_5(P + P_a)^{C_6}} \tag{17}$$

Table 2
Sigmoid and TTPS Shift model coefficients - AB11 Mixture.

Model	Coefficients									
	α	β	γ	δ	C_1	C_{20}	C_{21}	C_{30}	C_{31}	C_4
1	4.52	−0.06	−0.46	2.24	10.11	83.42	0.21	1.53	0.02	0.25
2	4.40	0.29	−0.68	2.61	8.92	99.11	0.99	0.96	1.50	5.17

Table 3
Sigmoid and TTPS Shift model coefficients - SKA11 Mixture.

Model	Coefficients									
	α	β	γ	δ	C_1	C_2	C_3	C_4	C_5	C_6
1	4.15	−0.81	−0.83	1.75	7.03	54.44	0.04	0.15	2.5E-03	92.27
2	4.12	−0.79	−0.85	1.77	6.85	54.5	2.0	2.0	2.2	4.9

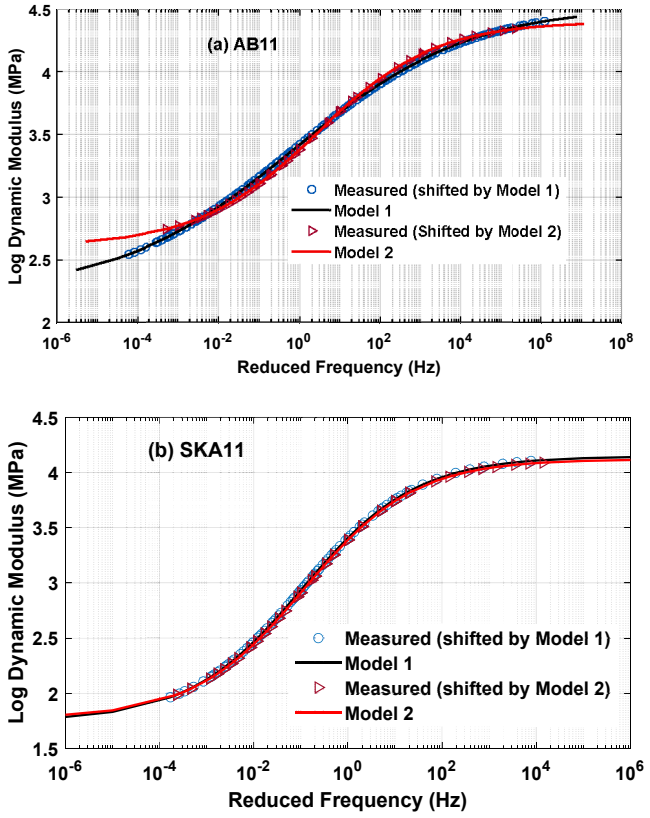

Fig. 4. Stress-dependent Master Curves at 21 °C and 100 kPa for AB11 and SKA11 Mixtures.

Where P_a is atmospheric pressure (101.3 kPa); C_3–C_6 are regression coefficients;P, P_o are confining and reference pressures, respectively.

All stress-dependent master curves in the subsequent sections are constructed at 21 °C reference temperature and 100 kPa reference confining pressure. A total of ten parameters (including four sigmoid parameters) were optimized to construct the stress-dependent master curves (see in Table 2 and Table 3).

In Fig. 4 a-b, the triaxial master curves are presented for AB11 and SKA11 mixtures. Both Model 1 and Model-2 have good prediction accuracy ($R^2 = 0.98$ for model-1 and $R^2 = 0.95$ for Model-2 for AB11) (as shown in Fig. 5). For the SKA11 mixture, a very close prediction is observed using both models (Fig. 4 b). It is seen that both models have the advantage of simplicity while successfully shifting stress-dependent master curves. Model 1 has a wider reduced frequency range and better accuracy than Model2. In addition, Model 1 is derived based on the free volume theory and has a sound physical and theoretical basis. On the other hand, Model 2 is a mathematical sigmoid function with a characteristic S-shaped. The vertical shift model is independently determined and added to the sigmoid model (i.e., the model is a two-step process). Hence, Model-1 is favored and proposed for further analyses in this paper with simplifaction. As shown in Fig. 6, the vertical shift factor $\Gamma(p)$ has an approximate linear function relationship with confining pressure.

5. Time-domain viscoelastic properties

Although the frequency domain dynamic modulus can give sufficient information about the viscoelastic properties of asphalt concrete, the time domain modulus is often used for performance prediction. Interconversion between frequency and time domain is performed using storage and loss modulus data. Often conversions based on the storage modulus data provide sufficient accuracy. But it is essential to evaluate the smoothness of storage modulus data before conversion to time-domain moduli. As shown in Fig. 3, the dissipated energy due to phase angle introduces noise and inconsistency to the storage modulus at high temperatures. Hence, a continuous sigmoidal function [13] in Eq. (18) is used to smoothen and avoid discreteness, wave or noise in the data. The error optimization function of $min[\log_{10}(E(f_R)) - g(f_R)]$ is used.

$$g(f_R) = a_1 + \frac{a_2}{a_2 + \frac{a_4}{exp(a_5 + a_6 log f_R)}} \tag{18}$$

Where $a_{1,\ 2,\ \ldots,\ 6}$ are coefficients, f_R is the reduced frequency. The filtered storage modulus data (as shown in Fig. 7) is then utilized to obtain relaxation modulus using the Prony method.

5.1. Relaxation modulus

The Prony function (Eq. (19)) [15] with error minimization objective function, OF (Eq. (20)) is used to predict the relaxation modulus from pre-smoothen storage modulus data.

$$E(\omega) = E_\infty + \sum_{m=1}^{M} \frac{\omega^2 \rho_m^2 E_m}{1 + \omega^2 \rho_m^2} \tag{19}$$

$$OF = \frac{1}{N}\left[\sum_{i=1}^{N}\left(1 - \frac{|E^*(\omega_i)|_{Predicted}}{|E^*(\omega_i)|_{Measured}}\right)^2\right] \tag{20}$$

Where E_∞ is long-term relaxation modulus (Mpa), E_m and ρ_m *are* Prony coefficients (relaxation modulus [MPa] and relaxation time [sec], ω is angular frequency, M is number of Prony coefficients of a generalized Maxwell model, and N is number of storage modulus data points.

The data presented in the subsequent sections are only for AB11 asphalt concrete. In Fig. 8, the isobaric and triaxial relaxation modulus

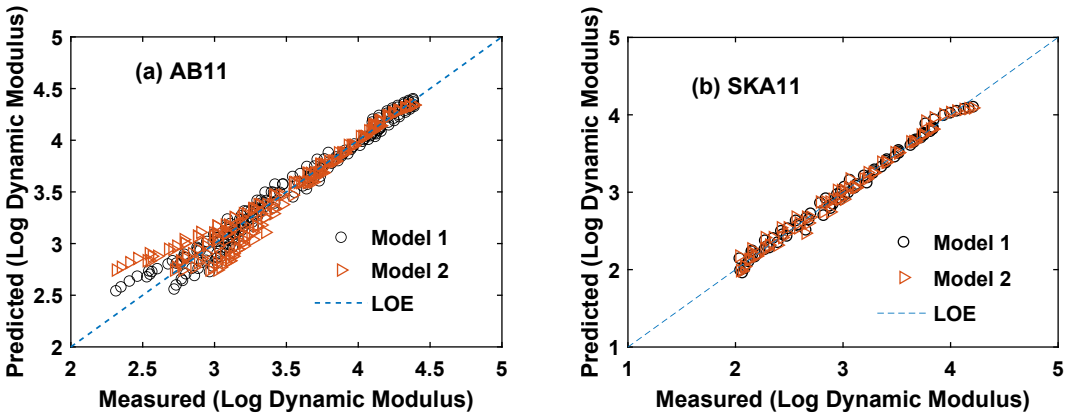

Fig. 5. Accuracy of Stress-dependent master curve predicting models for AB11 and SKA11 mixtures.

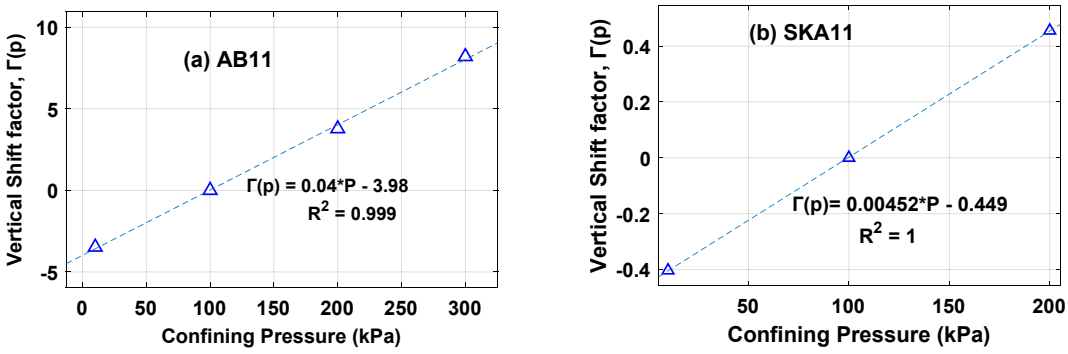

Fig. 6. Vertical shift factor versus confining Pressure (Model 1) for AB11 and SKA11 mixtures.

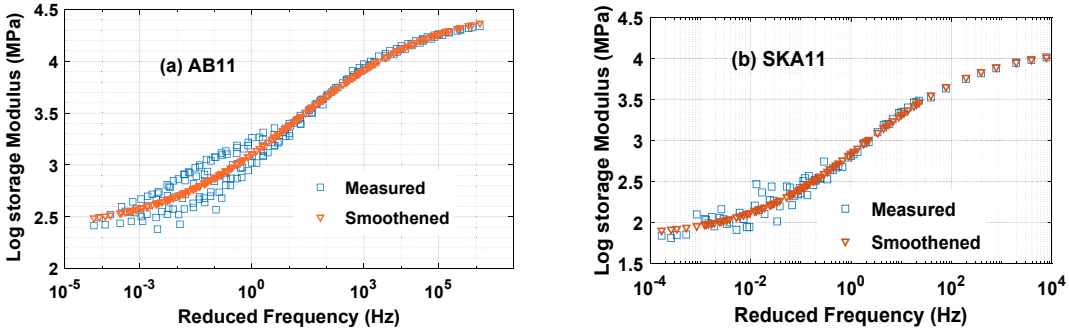

Fig. 7. Pre-smoothened Storage Modulus master curves.

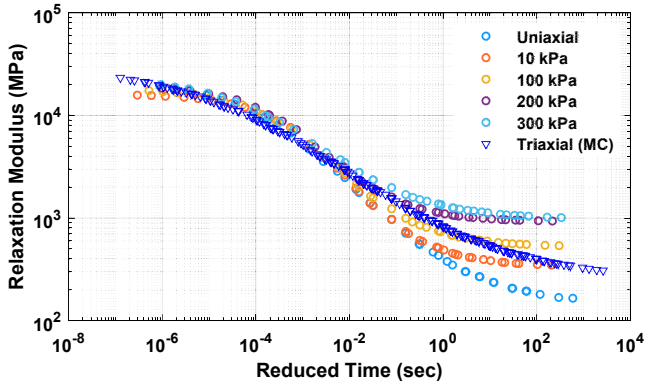

Fig. 8. Isobaric and triaxial Relaxation Modulus Master Curves – AB11 Mixture.

master curves using Model-1 are shown. It is seen that the effect of confining pressure is significant on the long-term side of the relaxation modulus. The Prony terms of a generalized Maxwell model presented in Fig. 9 and Table 4 showed a normal (Gaussian) distribution of relaxation moduli of the Prony coefficients. A total of twelve Prony coefficients were used. The coefficients (Ei) at long-time are almost the same and can be taken as independent of confining stress.

Furthermore, the bulk (volumetric) and shear moduli should be considered in the triaxial stress analysis for granular materials like asphalt concrete. From Eq. (5), it can be observed that the bulk relaxation modulus is more sensitive to change in Poisson ratio than the corresponding shear modulus. For incompressible materials (when $\upsilon = 0.5$), the bulk relaxation spectra (K_m) are zero or the bulk modulus $K(t)$ is infinite. To illustrate the relationship between the three moduli *(E, G and K)*, a parametric study at different constant Poisson ratios is shown in Fig. 10. For example, as Poisson ratio increases from 0.3 to 0.35, the shear modulus increases by 3.8%, and the bulk modulus is reduced by

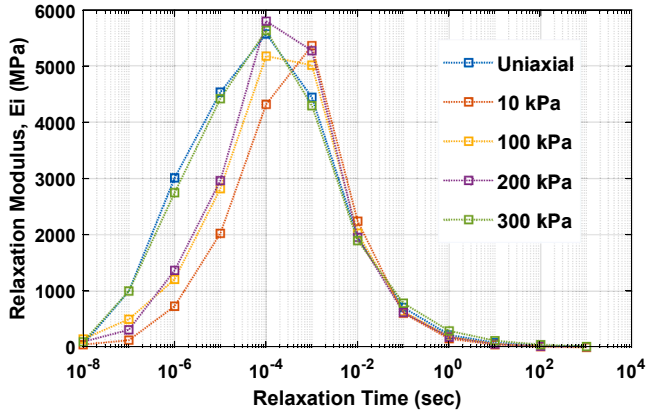

Fig. 9. Prony Coefficient Relaxation Moduli (Gaussian type distribution) – AB11 Mixture.

Table 4
Prony Coefficients of relaxation Spectrum.

		Confining Pressure [kPa]				
m	ρ_m [sec]	Uniaxial	10	100	200	300
1.	1.0E-08	49.93	50.00	148.88	99.91	99.90
2.	1.0E-07	1000.00	128.85	500.00	313.05	1000.00
3.	1.0E-06	3010.97	732.38	1210.12	1368.52	2746.72
4.	1.0E-05	4531.55	2025.15	2820.49	2962.72	4417.43
5.	1.0E-04	5566.01	4315.72	5173.00	5792.28	5628.03
6.	1.0E-03	4439.48	5359.20	5010.70	5268.25	4292.64
7.	1.0E-02	1956.16	2241.81	2027.36	1954.50	1896.97
8.	1.0E-01	708.32	607.34	638.67	621.62	786.14
9.	1.0E + 00	224.02	154.84	188.90	183.54	294.38
10.	1.0E + 01	83.97	48.50	64.21	60.77	120.83
11.	1.0E + 02	33.15	15.41	22.31	19.59	49.20
12.	1.0E + 03	18.12	0.01	1.79	9.94	18.09
E_∞ [MPa]		149.26	344.35	533.57	921.67	989.65

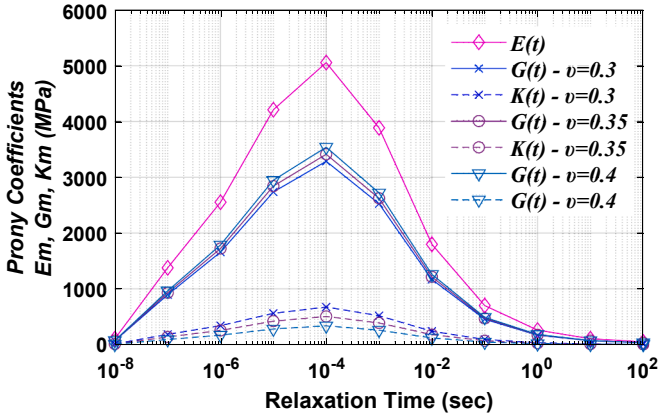

Fig. 10. Parametric study – relaxation, shear, and bulk Moduli at different Poisson ratios.

25%. Similarly, if the Poisson ratio increases from 0.35 to 0.4, the bulk modulus showed a 33% reduction and the shear component increased by 3.7%. As discussed previously, the applied confining pressure is expected to be lower than the minimum tensile strength of asphalt concrete. Thus, deformation caused by confining stress is assumed an elastic strain. Moreover, as temperature increases, tensile strength decreases contrary to the increment of the Poisson ratio. Therefore, the bulk modulus will ultimately be reduced and vanish due to high viscosity at $\upsilon = 0.5$ (incompressible).

5.2. The effect of confining pressure on viscoelastic damage parameter

For a viscoelastic material, the absolute maximum slope of the relaxation modulus curve is found confining stress-dependent. The maximum slope of the Log-Log relaxation modulus E(t) – time (t) curve is computed using the following expression.

$$S_o = \frac{d[logE(t)]}{dt} = \frac{\sum_{m=1}^{M}\left(-E_m \times e^{-\frac{t}{\rho_m}}\right)}{E_\infty + \sum_{m=1}^{M}\left(E_m \times e^{-\frac{t}{\rho_m}}\right)} \tag{21}$$

The maximum slope (S_o) is a crucial parameter for the viscoelastic damage prediction of asphalt concrete. The viscoelastic continuum damage parameter (α) is described as $\alpha = \frac{1}{S_o}$ for control-stress and $\alpha = \frac{1}{S_o}+1$ for control-strain fatigue damage modes [4,11]. As shown in Fig. 11a, the absolute maximum slope is reduced as confining pressure increases and due to the increment of relaxation modulus at an infinite time (or when frequency approaches zero, $\omega \cong 0$) on the high-temperature side. On the other hand, the damage parameter (α) increases as confining pressure increases much faster (5.4 times) than the slope (S_o) reduction rate (Fig. 11b). Conventionally, fatigue damage tests are uniaxial and ignored the role of triaxial (3D) stress conditions. It is revealed that the triaxial stress-state affects the damage evolution parameter and subsequently impacts the fatigue life prediction of asphalt concrete. Further research is underway on this topic by the authors of this paper. The role of confinement on the permanent deformation evolution is well understood and incorporated in the strain hardening phenomenon of asphalt concrete materials.

5.3. Effect of confining Pressure on the Long-term relaxation modulus

The long-term relaxation modulus (E_∞) is a modulus at a very long time ($t \to \infty$) or when the frequency approaches zero ($\omega \to 0$). After removing the applied load, the viscoelastic material gradually recovers its deformation, and full recovery is possible given sufficient time. The long-term relaxation modulus is the modulus that governs the stress relaxation of a material in the long-time limit. The relaxation modulus is a crucial quantity for performance prediction. From the sigmoid storage modulus [$log(E) = \delta + \frac{(\alpha-\delta)}{1+exp(\eta-\gamma log f_R)}$], the long-term relaxation modulus is the minimum value as frequency closes to zero (i.e., δ or $E_\infty \cong 10^{\delta}$). Different models have been proposed to correlate E_∞ with confining stress [16,28]. As shown in Fig. 9 and Fig. 12, the long-term relaxation modulus is dependent on confining stress and a linear relation can be seen between the long-term relaxation modulus and confining pressure.

There is a relatively weak correlation between the long-term relaxation modulus and the absolute maximum slope of the relaxation modulus curve and the damage parameter, as shown in Fig. 13.

5.4. Triaxiality ratio in linear viscoelastic response

In this paper, the stress ratio parameter (triaxiality ratio) is introduced to investigate the linear viscoelastic (LVE) property of asphalt concrete. The triaxiality ratio (η) is defined as the ratio of hydrostatic pressure (mean stress, σ_m) and the von Mises equivalent stress (σ_{vm}) or the ratio of the first stress invariant (I_1) to the second deviatoric stress invariant (J_2). It is argued that the stress ratio factor is essential to describe the stress-dependent LVE response of asphalt concrete.

$$\eta = \frac{\sigma_m}{\sigma_{vm}} = \frac{I_{1/3}}{\sqrt{3J_2}} \tag{22}$$

Where η is triaxiality ratio; $\sigma_m = \frac{\sigma_1+\sigma_2+\sigma_3}{3}$; $\sigma_{vm} = \sqrt{\frac{(\sigma_1-\sigma_2)^2+(\sigma_1-\sigma_3)^2+(\sigma_2-\sigma_3)^2}{2}}$; σ_1,σ_2, σ_3 are principal stresses. Simplifying Eq. (22) for triaxial condition, i.e., $\sigma_1 = \sigma_d + \sigma_c$ and $\sigma_2 = \sigma_3 = \sigma_c$ (σ_c is denotes confining pressure and σ_d is peak deviatoric stress) takes the following form.

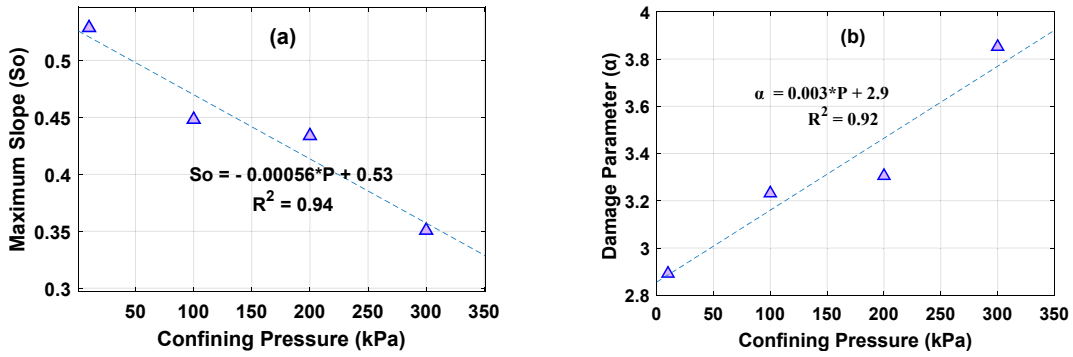

Fig. 11. Confining Pressure versus (a) Maximum slope (S_o) (b) Damage evolution Parameter (α).

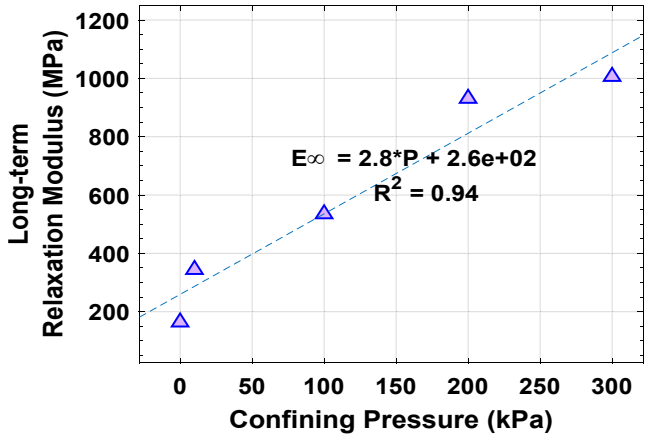

Fig. 12. Long-term relaxation Modulus at different confining pressures.

$$\eta = \frac{\sigma_c}{\sigma_d} + \frac{1}{3} \tag{23}$$

The triaxiality ratio for the uniaxial or unconfined ($\sigma_c = 0$) condition is 1/3. The ratio increases as the confinement level dominate the Mises equivalent stress. Theoretically, the maximum ratio (i.e.,$\eta = \infty$) is obtained when deviatoric stress is minimum or at very high hydrostatic stress.

The peak deviatoric stress is obtained from the frequency sweep dynamic modulus test. Fig. 14 shows the peak deviatoric stress in a strain-controlled triaxial dynamic modulus test. The stress decreases as temperature increases and frequency reduces. That means maximum deviatoric stress is exerted at low temperature and high frequency to maintain the target strain limit (50 micros). As can be seen in the figure, the peak deviatoric stress does not vary much with confining pressure at a particular test temperature. This confirms the consistency of applied deviatoric stress regardless of the different volumetric stresses. However, the slight variations observed (e.g., at 21 °C) could be due to transient effects during the sinusoidal test or due to lateral pressures. As shown in Fig. 15a-b, the triaxiality ratios are computed at each temperature and confining stress. It is clearly seen that η is both pressure and temperature-dependent, and increases with both confining pressure and temperature in a controlled-strain test. Furthermore, a power relationship (with R^2 over 0.95) is observed between η and the two thermodynamic variables (temperature and pressure). The rate of triaxiality ratio start decreasing from and after 100 kPa confinement (Fig. 15b) and 40 °C temperature (Fig. 15a). Although the realistic confining pressure in the asphalt pavement is not accurately known, the range between 100 and 250 is generally considered as an in-situ confining stress range (average of 150 to 175 kPa). The surface plot in Fig. 16 also shows that the triaxiality ratio is critical at the combination of hot temperature and high confinement conditions. This observation indirectly implies that the linearity limit of asphalt concrete depends on the triaxiality ratio (Von Mises and mean stresses) and can be determined using different combinations of confining pressures, temperatures, and deviatoric stresses. Based on the observations from Figs. 15 and 16, the triaxiality ratio can be integrated into the time-temperature-pressure shift model to predict triaxail stress-dependent LVE response of asphalt concrete.

5.5. The proposed model

The triaxiality ratio (η) is a fundamental material parameter that can couple the stress-dependent thermo-piezo-rheology responses of viscoelastic materials. The Prony method is widely used for viscoelastic modeling of asphalt concrete. From a mechanistic viewpoint, the triaxiality ratio is more comprehensive and efficient approach to model triaxial viscoelastic properties. As discussed in **Section 5.4**, the triaxiality ratio (η) is dependent on both temperature and pressure. This paper proposes a new model to integrate the triaxiality ratio with the time–temperature-pressure superposition principle. The proposed model takes the following form.

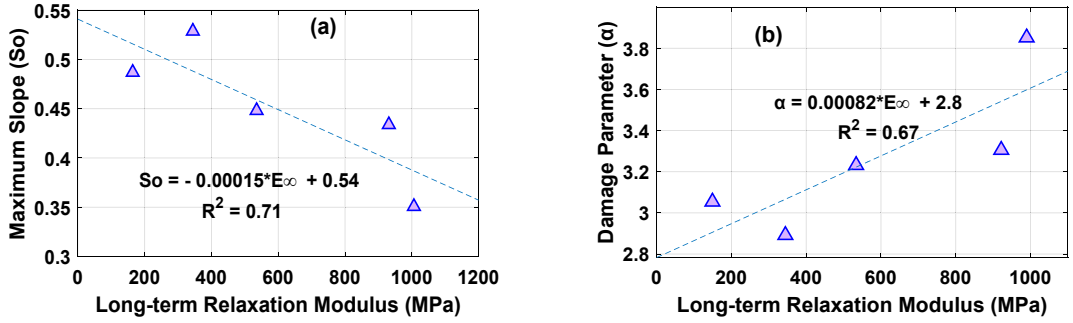

Fig. 13. Long-term relaxation Modulus versus Maximum slope and viscoelastic damage parameter.

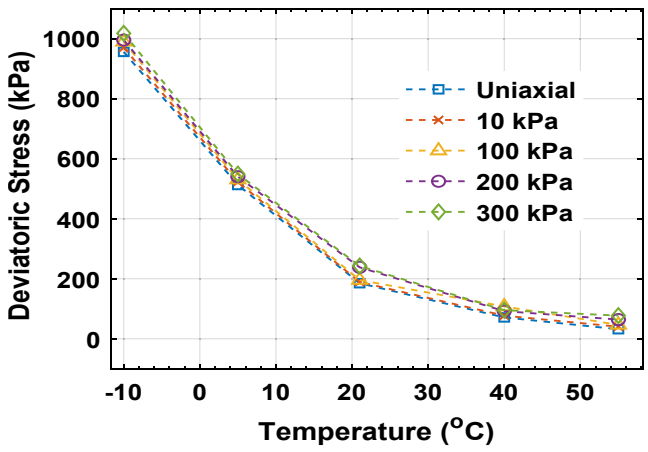

Fig. 14. Peak deviatoric stress at different Confining Pressures and temperatures.

$$log\alpha_{TP} = \frac{-C_1[T - T_0 - \Gamma(p)]}{C_{22} + C_{23}\eta + T - T_0 - \Gamma(p)} \tag{24}$$

$$\Gamma(p) = (C_7\eta)ln\left(\frac{1 + C_8P}{1 + C_8P_0}\right) \tag{25}$$

Where $C_1, C_{22}, C_{23}, C_7, C_8$ are temperature and pressure shift factor coefficients. A master curve is constructed using the new proposed model (Eqs. (24) and (25)) and compared with Model-1 (Eqs. (13), 15, and 16). As shown in Fig. 17, the proposed triaxiality ratio-based model fitted the measure data well. The main advantage of this model is the consideration of deviatoric stress in the LVE modeling while being concise and fewer number of model coefficients. In most dynamic modulus tests, the load control mechanism is controlled-strain modes. Limiting the strain output is more controllable than that of the stress when linear viscoelastic response is concerned. However, there are circumstances where stress-controlled responses can be more plausible. In such conditions, the proposed triaxiality ratio shift model is convinient to predict the linear viscoelastic response.

Furthermore, the relationship between the long-term relaxation modulus (E_∞) and the triaxiality ratio (η) is established.

$$E_\infty = 10^{[\kappa + \lambda \times \ln(\eta)]} \tag{26}$$

Where κ and λ are fitting parameters. The exponent in Eq. (26) is equivalent to the minimum dynamic modulus value δ of the sigmoid function i.e., $min[log(E^*)] = \delta = \kappa + \lambda \times \ln\eta$). As shown in Fig. 18, a good correlation is observed between long-term relaxation modulus (E_∞) and the triaxiality ratio (η) at high temperatures. This is because the stress ratio is more critical on the viscous side of asphalt concrete than the elastic part (as shown in Fig. 16). The fitting parameters of the model (Eq. (26)) are given in Table 5.

6. Conclusion

In this paper, the effect of triaxial stress on the linear viscoelastic properties of asphalt concrete material was investigated using triaxial dynamic modulus test over a wide range of temperatures, frequencies, and confining stresses. Two different asphalt mixtures (neat and polymer-modified binder) were used and proved as thermo-piezo-rheologically simple material. The Fillers, Moonan, and Tschoegl (FMT) model is adopted for time–temperature-Pressure shifting and compared with another model from literature (Model 2). The stress ratio concept (triaxiality ratio) is introduced to characterize the stress-dependent viscoelastic properties of asphalt concrete. The main contributions are summarized as follows.

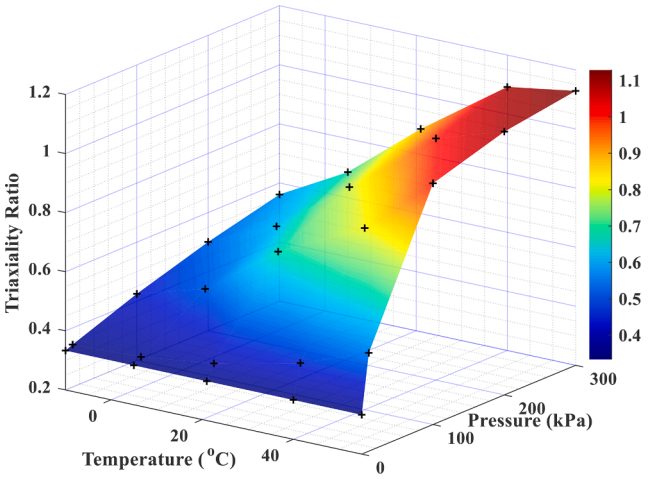

Fig. 16. Three-dimensional Surface plot of Triaxiality ratio.

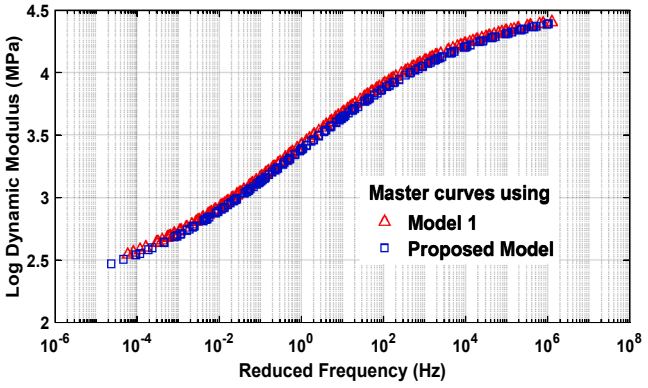

Fig. 17. Triaxial Master curves using Model-1 and the New Triaxial Ratio-based model.

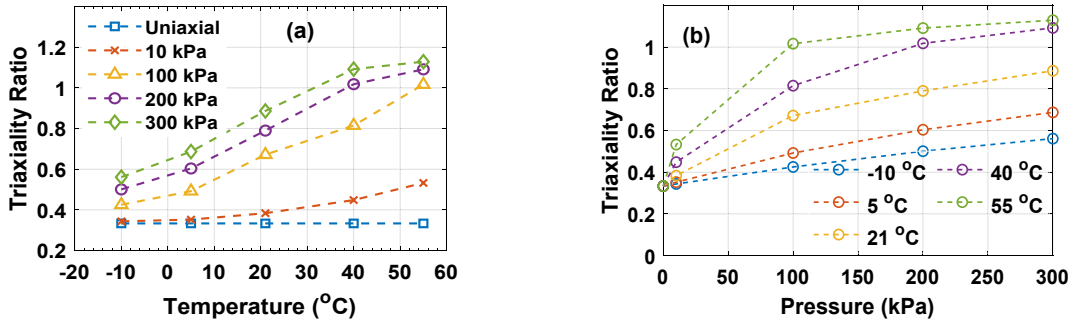

Fig. 15. Triaxiality ratio at different Confining Pressures and Temperatures.

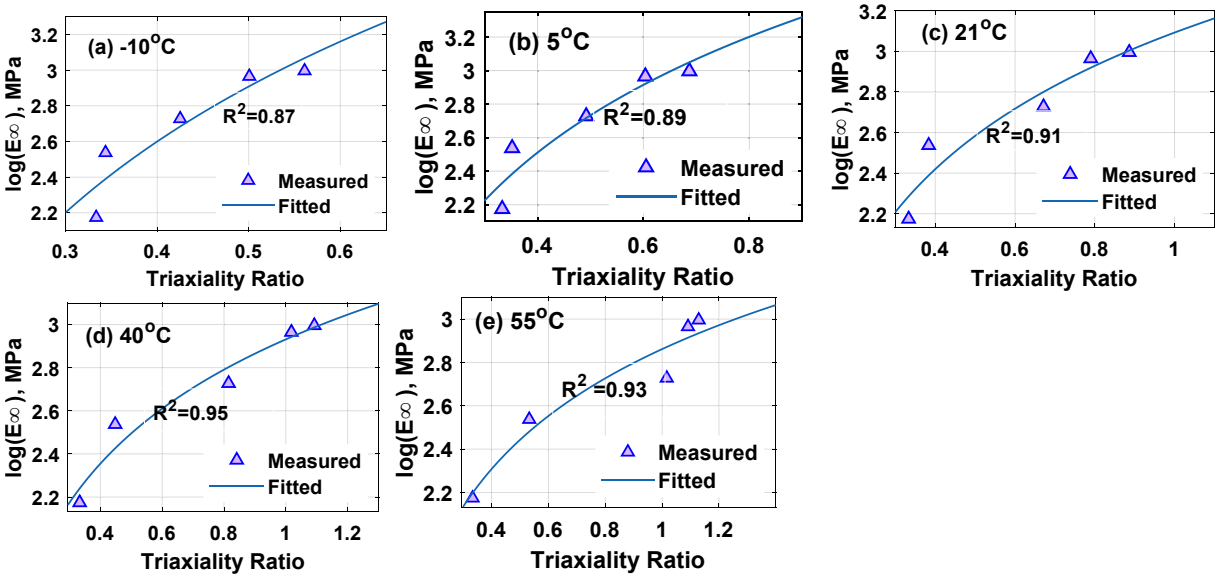

Fig. 18. Triaxiality ratio versus long-term relaxation modulus at different pressure and temperatures.

Table 5
Fitting Parameters for Eq. (26).

Coefficient	Temperature [°C]				
	−10	5	21	40	55
κ	3.87	3.42	3.09	2.93	2.86
λ	1.38	1.00	0.73	0.63	0.60

- The linear viscoelastic (LVE) property of asphalt concrete in a triaxial stress state is validated using the time–temperature-pressure superposition principle (TTPSP). The LVE properties are highly stress-dependent at intermediate and high temperatures.
- A simplified, integral (one-step), and theoretically sound vertical shift model is proposed by modifying the FMT model to construct triaxial master curves.
- A Prony method time-domain viscoelastic analysis revealed that the long-term relaxation modulus and maximum slope of a relaxation modulus curve are strongly stress-dependent. However, the Prony series coefficients (Ei) are independent of pressure at high relaxation time.
- A slight reduction of the maximum slope of relaxation modulus due to confining pressure causes more than 5.4 times increment of the viscoelastic fatigue damage parameter, highlighting the limitations of uniaxial fatigue life prediction, particularly at intermediate temperatures (from 15 to 25).
- The concept of triaxiality ratio is introduced to characterize the 3D stress effect on the linear viscoelastic responses of asphalt concrete. For a controlled-strain dynamic modulus test, the triaxiality ratio increases with temperature and pressure. In addition, the ratio has a strong correlation with the long-term relaxation modulus.
- A new triaxial TTPSP shifting model is proposed and validated. The triaxiality ratio can indirectly characterize the viscoelastic linearity limit for the thermo-piezo-rheological simple materials.

CRediT authorship contribution statement

Mequanent Mulugeta Alamnie: Conceptualization, Methodology, Data curation, Writing – original draft, Visualization. **Ephrem Taddesse:** Conceptualization, Supervision. **Inge Hoff:** Supervision.

Declaration of Competing Interest

The authors declare that they have no known competing financial interests or personal relationships that could have appeared to influence the work reported in this paper.

Appendix A. Supplementary data

Supplementary data to this article can be found online at https://doi.org/10.1016/j.conbuildmat.2022.127106.

References

[1] J. Blanc, T. Gabet, P. Hornych, J.-M. Piau, H. di Benedetto, Cyclic triaxial tests on bituminous mixtures, Road Mater. Pavement Des. 16 (2014) 46–69.
[2] W. Cao, Y.R. Kim, A viscoplastic model for the confined permanent deformation of asphalt concrete in compression, Mech. Mater. 92 (2016) 235–247.
[3] G. Chehab, Y. Kim, R. Schapery, M. Witczak, R. Bonaquist, Time-temperature superposition principle for asphalt concrete with growing damage in tension state, J. Assoc. Asphalt Paving Technol. 71 (2002).
[4] J.S. Daniel, Y.R. Kim, Development of a simplified fatigue test and analysis procedure using a viscoelastic, continuum damage model (with discussion), J. Assoc. Asphalt Paving Technol. 71 (2002).
[5] M.K. Darabi, R.K. Abu Al-Rub, E.A. Masad, C.-W. Huang, D.N. Little, A thermo-viscoelastic–viscoplastic–viscodamage constitutive model for asphaltic materials, Int. J. Solids Struct. 48 (2011) 191–207.
[6] EMRI, I. 2005. Rheology of solid polymers. *Rheology Reviews,* 2005, 49.
[7] J.D. Ferry, R.A. Stratton, The free volume interpretation of the dependence of viscosities and viscoelastic relaxation times on concentration, pressure, and tensile strain, Kolloid-Zeitschrift 171 (1960) 107–111.
[8] R.W. Fillers, N.W. Tschoegl, The Effect of Pressure on the Mechanical Properties of Polymers, Trans. Soc. Rheol. 21 (1977) 51–100.
[9] W.N. Findley, J.S. Lai, K. Onaran, Creep and relaxation of nonlinear viscoelastic materials, North-Holland Publishing, 1976.
[10] P. Gayte, H. di Benedetto, C. Sauzéat, Q.T. Nguyen, Influence of transient effects for analysis of complex modulus tests on bituminous mixtures, Road Mater. Pavement Des. 17 (2016) 271–289.
[11] H.-J. Lee, J.S. Daniel, Y.R. Kim, Continuum Damage Mechanics-Based Fatigue Model of Asphalt Concrete, J. Mater. Civ. Eng. 12 (2000) 105–112.
[12] W.K. Moonan, N.W. Tschoegl, The effect of pressure on the mechanical properties of polymers. IV. Measurements in torsion, J. Polym. Sci.: Polym. Physics Ed. 23 (1985) 623–651.
[13] S. Mun, G.R. Chehab, Y.R. Kim, Determination of Time-domain Viscoelastic Functions using Optimized Interconversion Techniques, Road Mater. Pavement Des. 8 (2007) 351–365.
[14] M.L. Nguyen, C. Sauzéat, H. di Benedetto, N. Tapsoba, Validation of the time–temperature superposition principle for crack propagation in bituminous mixtures, Mater. Struct. 46 (2013) 1075–1087.
[15] Park, S. W. & Schapery, R. A. 1999. Methods of interconversion between linear viscoelastic material functions. Part I—a numerical method based on Prony series. 36, 1653-1675.

[16] T.K. Pellinen, M.W. Witczak, M. Marasteanu, G. Chehab, S. Alavi, R. Dongré, Stress dependent master curve construction for dynamic (complex) modulus. Asphalt Paving Technology: Association of Asphalt Paving Technologists-Proceedings of the Technical Sessions, Association of Asphalt Paving Technologist, 2002, pp. 281–309.
[17] D. Perraton, H. di Benedetto, C. Sauzéat, B. Hofko, A. Graziani, Q.T. Nguyen, S. Pouget, L.D. Poulikakos, N. Tapsoba, J. Grenfell, 3Dim experimental investigation of linear viscoelastic properties of bituminous mixtures, Mater. Struct. 49 (2016) 4813–4829.
[18] E. Rahmani, M.K. Darabi, R.K. Abu Al-Rub, E. Kassem, E.A. Masad, D.N. Little, Effect of confinement pressure on the nonlinear-viscoelastic response of asphalt concrete at high temperatures, Constr. Build. Mater. 47 (2013) 779–788.
[19] N. Roy, A. Veeraragavan, J.M. Krishnan, Influence of confinement pressure and air voids on the repeated creep and recovery of asphalt concrete mixtures, Int. J. Pavement Eng. 17 (2016) 133–147.
[20] C.W. Schwartz, N. Gibson, R.A. Schapery, Time-Temperature Superposition for Asphalt Concrete at Large Compressive Strains, Transp. Res. Rec.: J. Transp. Res. Board 1789 (2002) 101–112.
[21] Y. Sun, B. Huang, J. Chen, X. Shu, Y. Li, Characterization of Triaxial Stress State Linear Viscoelastic Behavior of Asphalt Concrete, J. Mater. Civ. Eng. 29 (2017) 04016259.
[22] N.W. Tschoegl, Energy Storage and Dissipation in a Linear Viscoelastic Material, in: N.W. Tschoegl (Ed.), The Phenomenological Theory of Linear Viscoelastic Behavior, Springer Berlin Heidelberg, Berlin, Heidelberg, 1989.
[23] N.W. Tschoegl, Time Dependence in Material Properties: An Overview, Mech. Time-Dependent Mater. 1 (1997) 3–31.
[24] J. Uzan, Characterization of Asphalt Concrete Materials for Permanent Deformation, Int. J. Pavement Eng. 4 (2003) 77–86.
[25] M.L. Williams, R.F. Landel, J.D. Ferry, The temperature dependence of relaxation mechanisms in amorphous polymers and other glass-forming liquids, J. Am. Chem. Soc. 77 (1955) 3701–3707.
[26] T. Yun, B.S. Underwood, Y.R. Kim, Time-Temperature Superposition for HMA with Growing Damage and Permanent Strain in Confined Tension and Compression, J. Mater. Civ. Eng. 22 (2010) 415–422.
[27] Y. Zhang, R. Luo, L. Lytton Robert, Anisotropic Viscoelastic Properties of Undamaged Asphalt Mixtures, J. Transp. Eng. 138 (2012) 75–89.
[28] Y. Zhao, H. Liu, W. Liu, Characterization of linear viscoelastic properties of asphalt concrete subjected to confining pressure, Mech. Time-Dependent Mater. 17 (2013) 449–463.
[29] Y. Zhao, Y. Richard Kim, Time–Temperature Superposition for Asphalt Mixtures with Growing Damage and Permanent Deformation in Compression, Transp. Res. Rec.: J. Transp. Res. Board 1832 (2003) 161–172.
[30] Y. Zhao, J. Tang, H. Liu, Construction of triaxial dynamic modulus master curve for asphalt mixtures, Constr. Build. Mater. 37 (2012) 21–26.